

Mapping the Fermi velocity in the quasi-2D organic conductor κ -(BEDT-TTF)₂I₃

A. E. Kovalev,¹ S. Hill,^{1,*} K. Kawano,² M. Tamura,^{2,†} T. Naito,³ and H. Kobayashi⁴

¹*Department of Physics, University of Florida, Gainesville, FL 32611, USA*

²*Toho University, Funabashi, 274-8510, Japan*

³*Hokkaido University, Sapporo, 060-0810, Japan*

⁴*Institute for Molecular Science, Okazaki, Aichi 444-8585, Japan*

(Dated: November 18, 2018)

We demonstrate a new method for determining the Fermi velocity in quasi-two-dimensional (Q2D) organic conductors. Application of a magnetic field parallel to the conducting layers results in periodic open orbit quasiparticle trajectories along the Q2D Fermi surface. Averaging of this motion over the Fermi surface leads to a resonance in the interlayer microwave conductivity. The resonance frequency is simply related to the extremal value of the Fermi velocity perpendicular to the applied field. Thus, angle dependent microwave studies enable a complete mapping of the Fermi velocity. We illustrate the applicability of this method for the highly-2D organic conductor κ -(BEDT-TTF)₂I₃.

PACS numbers: 71.18.+y, 72.15.Gd, 74.70.Kn, 76.40.+b

Microwave spectroscopy has been utilized as a means of studying the electrodynamic properties of metals for well over half a century, especially resonant absorption in an external DC magnetic field. Quasiparticles in such conductors usually move on closed periodic trajectories in reciprocal (k -) space, or cyclotron orbits in real space (we will always consider the motion in k -space, unless stated otherwise). When any period associated with this motion matches the period of the external electromagnetic field, so-called cyclotron resonance (CR) occurs if the condition $\omega_c \tau > 1$ is satisfied, where ω_c is the cyclotron frequency and τ is the relaxation time; ω_c depends on the magnetic field strength, and on the cyclotron mass (m_c) – a characteristic of the Fermi surface (FS) of the metal. In conventional metals, large Fermi velocities ($v_F \sim 10^6$ m/s) complicate matters to the extent that CR is normally only observed in the anomalous skin effect regime. The theoretical foundations for this and many other electrodynamic properties of metals have been firmly established [1].

In layered organic conductors, the FS may be either quasi-two-dimensional (Q2D), quasi-one-dimensional (Q1D), or a combination of both. In the Q2D case, the FS is a warped cylinder with its axis perpendicular to the layers (see Fig. 1) while, in the Q1D case, the FS consists of a pair of warped sheets at $\pm k_F$. Because of this reduced dimensionality (and reduced $v_F \sim 10^5$ m/s) several new effects in the microwave conductivity have been reported. One of these is the observation of multiple periodic orbit resonances (POR) in Q1D systems [2, 3, 4, 5]. In this situation, quasiparticles move under the external magnetic field along open orbits. The motion is periodic because of the underlying periodicity of the crystal lattice. When the period of this motion coincides with the period of an appropriately polarized electromagnetic field, resonant microwave absorption occurs, *i.e.* the AC conductivity attains a maximum. Recent studies have shown that multiple POR harmonics

may be observed, each one corresponding to a different fourier component of the warping of the Q1D FS [5]. The POR frequencies are simply related to the magnetic field strength, the crystal lattice parameters, and the Q1D Fermi velocity (v_F). Indeed, this effect provides the most direct method of measuring v_F in a Q1D system, without making any assumptions about the underlying bandstructure [5].

Although a form of closed orbit CR has been reported for several Q2D organic conductors, its origin is quite different from that in normal metals [2, 6]. Electromagnetic fields penetrate easily into the bulk of the sample for current excitation normal to the layers [7], due to the very low conductivity in this direction (the anomalous skin effect is impossible to achieve in the millimeter spectral range, even for the highest conducting direction); the typical interlayer skin depth at 50 GHz is about 50 – 100 μ m, *i.e.* comparable with the sample dimensions. Indeed, typical sample shapes and conductivity anisotropies result in a situation wherein the interlayer conductivity (σ_{zz}) usually dominates the electrodynamic response [7]. Thus, it has been shown both theoretically [2, 6] and experimentally that the Q2D closed orbit resonances are related to the finite warping of the FS, *i.e.* this effect is analogous to the Q1D POR, albeit that the periodic motion normal to the layers is related to the underlying cyclotron motion which is predominantly confined to within the layers.

A new effect appears if one aligns the magnetic field within the layers of a Q2D conductor, *i.e.* perpendicular to the Q2D FS cylinder. In this case, the quasiparticle motion is *principally* open (except for a small fraction of the total electrons – see Fig. 1a). This results in periodic motion along open orbits normal to the layers. The period of this motion depends on the magnetic field strength, B , and the velocity component (v_\perp) perpendicular to the field. Consequently, the period depends strongly on the in-plane wavevector k_{xy} . However, as we

will show, averaging over the FS leads to the result that the extremal perpendicular velocity (v_{\perp}^{ext}) dominates the electrodynamic response, giving rise to a singularity (a form of resonance) in the interlayer conductivity. The resonance occurs when the period of the electromagnetic field matches the periodicity of these extremal quasiparticle trajectories. Thus, one can map out the Fermi velocity by this method. This effect was originally predicted by Peschanskii and Pantoja [8], albeit within the anomalous skin effect regime. In the following, we derive some expressions for the real experimental case, where the skin depth is bigger or comparable to the sample size. Using these calculations, we show that it is also possible to map out the Fermi velocity in this limit.

We consider an energy dispersion of the form:

$$E(\vec{k}) = \frac{\hbar^2 k_x^2}{2m_x} + \frac{\hbar^2 k_y^2}{2m_y} - 2t_{\perp} \cos(\vec{k} \cdot \vec{R}), \quad (1)$$

where m_x and m_y are the in-plane diagonal components of the effective mass tensor, \vec{R} is the real space vector characterizing the interlayer FS warping, and $4t_{\perp}$ is the interlayer bandwidth. For a calculation of the interlayer AC conductivity [$\sigma_{zz}(\omega)$] we use the Boltzmann transport equation:

$$\sigma_{zz}(\omega) = \frac{e^2}{4\pi^3} \int d^3\vec{k} \left[-\frac{\partial f_0(\vec{k})}{\partial E(\vec{k})} \right] v_z(\vec{k}, 0) \times \int_{-\infty}^0 v_z(\vec{k}, t) e^{-i\omega t} e^{t/\tau} dt, \quad (2)$$

where τ is the quasiparticle relaxation time. First, we assume a $T = 0$ limit, so that the derivative of the distribution function, $f_0(\vec{k})$, may be replaced by $\delta[E_F - E(\vec{k})]$, where E_F is the Fermi energy. Second, we neglect the part of the Lorentz force which depends on the interlayer velocity, v_z . Finally, we neglect the effect of the closed orbits. This assumption is valid provided $\sqrt{E_F/4t_{\perp}} \gg \tau/T_P$, where T_P is the smallest period

for the open orbits [9, 10]. From available Shubnikov-de Haas (SdH) and de Haas-van Alphen (dHvA) data for the title compound, the ratio $E_F/4t_{\perp}$ is estimated to be larger than 10^4 , *i.e.* κ -(BEDT-TTF)₂I₃ is highly two-dimensional. As we show later, τ/T_P is of order unity; thus, the closed orbits may be neglected. As a result, the interlayer conductivity can be written:

$$\sigma_{zz}(\omega) \propto \int_0^{\omega_c^{ext}} \frac{1}{|v_F|} \frac{dS_k}{d\omega_c} \frac{1 - i\omega\tau}{(1 - i\omega\tau)^2 + (\omega_c\tau)^2} d\omega_c, \quad (3)$$

where dS_k is an element on the FS, $\omega_c = eBav_{\perp}/\hbar$ is the frequency associated with a given quasiparticle trajectory on the FS, and ω_c^{ext} is the extremal value of ω_c (a is the interlayer spacing, and v_{\perp} is the in-plane velocity perpendicular to the applied magnetic field).

Looking at Eq. 3, one can see that $\sigma_{zz}(\omega)$ will be dominated by the extremal perpendicular velocity v_{\perp}^{ext} (see Fig. 1b), since $dS_k/d\omega_c$ diverges (*i.e.* $d\omega_c/dS_k \rightarrow 0$) at these points on the FS. This leads to a resonance condition whenever $\omega = \omega_c^{ext} (\equiv eBav_{\perp}^{ext}/\hbar)$, provided that $\omega\tau > 1$. Measurement of ω_c^{ext} , as a function of the field orientation ψ within the xy -plane, yields a polar plot of $v_{\perp}^{ext}(\psi)$. The procedure for mapping the Fermi velocity is then identical to that of reconstructing the FS of a Q2D conductor from the measured periods of Yamaji oscillations [11]. Analytically, assuming one can measure $v_{\perp}^{ext}(\psi)$, it is then possible to generate the Fermi velocity $v_F(\phi)$ using the following transformations (see also Fig. 1b):

$$v_F = \sqrt{(v_{\perp}^{ext})^2 + v_{\parallel}^2}; \quad \phi = \psi + \arctan\left(\frac{v_{\perp}^{ext}}{v_{\parallel}}\right);$$

$$v_{\parallel} = -\frac{dv_{\perp}^{ext}}{d\psi}. \quad (4)$$

One may also calculate the conductivity explicitly from Eq. 3, for the parabolic energy dispersion given in Eq. 1:

$$\sigma_{zz}(\omega, B, \psi) = \sigma_{zz}(0) \frac{1}{\sqrt{(1 - i\omega\tau)^2 + (v_{xm}^2 \sin^2 \psi + v_{ym}^2 \cos^2 \psi)(\frac{eaB}{\hbar}\tau)^2}}. \quad (5)$$

Here, $\vec{B} = (B \cos \psi, B \sin \psi, 0)$, and v_{xm} & v_{ym} are the maximal Fermi velocities along x and y respectively. For a magnetic field sweep, the resonance condition becomes $B_{res} = \hbar\omega/ea\sqrt{(v_{xm}^2 \sin^2 \psi + v_{ym}^2 \cos^2 \psi)}$.

To observe this new type of POR, we chose the highly-

2D organic superconductor κ -(BEDT-TTF)₂I₃ [12]. Its FS may be calculated using a 2D tight binding model, resulting in a network of overlapping Fermi cylinders [13], as shown in Fig. 1c. The lattice periodicity results in a removal of the degeneracy at the points where the cylinders cross each other. Thus, the actual FS consists of a small

Q2D pocket (dark shaded area in Fig. 1c) and a pair of Q1D open sections. However, the energy barrier separating these bands is relatively small, leading to magnetic breakdown at fairly low fields. Indeed, SdH and dHvA measurements [14] are dominated by the large breakdown orbit (lightly shaded area in Fig. 1c). Meanwhile, microwave studies with the field oriented perpendicular to the layers show very clear closed-orbit POR from both Q2D sections of the FS without any noticeable evidence for the Q1D part [15].

A small platelet shaped ($\sim 0.7 \times 0.4 \times 0.12 \text{ mm}^3$) single crystal of κ -(BEDT-TTF) $_2\text{I}_3$ was studied using a phase sensitive cavity perturbation technique (described elsewhere [16]). The sample was placed on the endplate of a cylindrical TE $_{011}$ cavity, and field rotation in a plane perpendicular to the axis of the cavity (\parallel highly conducting bc -plane of the sample) was achieved using a 7 T split-pair superconducting magnet. All measurements were carried out at $T = 4.5 \text{ K}$, above the superconducting transition temperature ($T_c = 3.5 \text{ K}$), and at a frequency of 53.9 GHz. According to published resistivity data [13], we estimate a 54 GHz skin depth for currents perpendicular (parallel) to the layers of 53 μm (4 μm). Thus, we expect σ_{zz} to dominate the losses in the cavity [7], as required in order to detect the new open orbit resonance.

In Fig. 2 we plot the field dependence of the microwave absorption and phase shift (solid curves) for several field orientations (ψ) within the highly conducting bc -plane of the sample. To understand the shapes of the curves, we treat the sample as a thin conducting plate of thickness d , subjected to a microwave AC magnetic field polarized within the plane of the plate. In this situation, the effective polarizability of the sample has the form:

$$\alpha(\omega) = \frac{\tanh(kd/2)}{kd/2} - 1, \quad (6)$$

where $k = (-i\omega\sigma\mu_0)^{1/2}$. The absorption is then proportional to the imaginary part of the $\alpha(\omega)$, while the phase shift is proportional to the real part. While Eq. 6 is clearly only approximate, we find excellent agreement between the predicted and observed behavior; as an illustration, we have included fits to the $\psi = -54^\circ$ data in Fig. 2. The resonances are rather broad (indicated by arrows), due to the fairly small $\omega\tau$ product (~ 2). While it is quite difficult to accurately determine the resonance position from the absorption data, it is relatively easy to do so using the phase shift.

In the Fig. 3 we plot the experimentally determined $v_\perp^{\text{ext}}(\psi)$ on a polar diagram. These values were deduced by three different methods: 1) from the maximum in the phase shift (\bullet); 2) from fits to the absorption curves (\circ); and 3), from fits to the phase shift curves ($*$). The dashed line is a fit to the points deduced by method 1, and the solid line is the corresponding Fermi velocity (from Eq. 4). The value for v_{xm} is $1.3 \times 10^5 \text{ m/s}$ and v_{ym}

is $0.62 \times 10^5 \text{ m/s}$. This anisotropy is in good agreement with the known anisotropy of the small Q2D FS for κ -(BEDT-TTF) $_2\text{I}_3$ (dark shaded region in Fig. 1c). If one assumes a parabolic dispersion (Eq. 1), it is possible to compare our data with the band parameters determined for the large Q2D β -orbit from optical data by Tamura *et al.* [17]. In particular, we may estimate the effective mass along the c -direction as $m_c^\beta = \hbar k_F^c / v_{xm} \sim 2.5m_e$, which compares to the value of $2.4m_e$ determined from the optical measurements [17].

Based on the known value, $S_k = 5.5 \times 10^{18} \text{ m}^{-2}$, for the area of the small Q2D section of the FS in k -space, we may estimate the momentum averaged cyclotron mass from the relation $m^* = \hbar(S_k/S_v)^{1/2}$, where S_v is the area of the FS in velocity space (Fig. 3). This method gives $m^* \approx 1.7m_e$, while the experimental value deduced from the SdH and dHvA effects is $\sim 1.9m_e$ [14], where m_e is the free electron mass; the value deduced from earlier closed orbit POR measurements is $2.2m_e$ [15]. The mass anisotropy (m_x/m_y) deduced from the present measurements for the small Q2D FS (dark shaded region in Fig. 1c) is 4. From fits to the data, we also estimate a relaxation time of $\tau \sim 5 \text{ ps}$, or $\omega\tau \sim 2$. Thus, our initial assumption to neglect closed orbits is fully justified.

In principle, one should also expect an open orbit resonance effect from the Q1D FS sections (see Fig. 1c), as has recently been reported for several other low-dimensional organic conductors [4, 5]. However, no clear evidence for such behavior was found. Indeed, our current and earlier [15] microwave studies clearly show that the Q2D FS dominates the electrodynamic properties of κ -(BEDT-TTF) $_2\text{I}_3$. This likely suggests that the warping of Q1D FS is weaker than that of the Q2D section.

Finally, we comment on the effect of a possible misalignment of the field rotation axis. Following Peschansky and Kartsovnik [10], we may assume that the conductivity will be dominated by the periodic motion along k_z , rather than by any cyclotron motion in the $k_x k_y$ -plane, provided $\sin\theta \ll 1/\omega_c^{\text{ext}}\tau$ (θ is the mis-alignment angle). Clearly, therefore, the accuracy of our sample alignment is enough to justify our procedure for mapping the Fermi velocity.

In conclusion, we have demonstrated a new type of magneto-electrodynamic resonance in a layered conductor with a Q2D FS. The resonance is observed for a magnetic field applied parallel to the layers, resulting in periodic open quasiparticle trajectories normal to the layers. The resonance frequency is simply related to the extremal value of the Fermi velocity perpendicular to the applied field. Thus, by rotating the field within the layers, one can map out the angle dependence of the Fermi velocity. We illustrate the applicability of this method for the highly-2D organic conductor κ -(BEDT-TTF) $_2\text{I}_3$, for which we obtain FS parameters which are consistent with published results.

This work was supported by the NSF (DMR0196430,

DMR0196461 and DMR0239481). S. H. would like to thank the Research Corporation for financial support.

* Electronic address: hill@phys.ufl.edu

† New address: RIKEN, Wako, Saitama 351-0198, Japan

- [1] A. A. Abrikosov, *Fundamentals of the theory of metals* (Elsevier, Amsterdam, 1988).
- [2] S. Hill, Phys. Rev. B **55**, 4931 (1997).
- [3] S. J. Blundell, A. Ardavan, and J. Singleton, Phys. Rev. B **55**, R6129 (1995).
- [4] A. Ardavan et al., Phys. Rev. Lett. **81**, 713 (1998).
- [5] A. E. Kovalev, S. Hill, and J. S. Qualls, Phys. Rev. B **66**, 134513 (2002).
- [6] R. H. McKenzie and P. Moses, Phys. Rev. B **60**, 11241 (1999).
- [7] S. Hill, Phys. Rev. B **62**, 8699 (2000).
- [8] V. G. Peschansky and J. C. M. Pantoja, Low Temperature Physics **26**, 494 (2000).
- [9] A. J. Shoenfield and J. R. Cooper, Phys. Rev. B **62**, 10 779 (2000).
- [10] V. G. Peschansky and M. V. Kartsovnik, Phys. Rev. B **60**, 11207 (1999).
- [11] M. Kartsovnik et al., J. Physique I **2**, 89 (1992).
- [12] R. Kato et al., Chem. Lett. p. 507 (1987).
- [13] H. Kobayashi et al., J. Mater. Chem. **5**, 1681 (1995).
- [14] E. Balthes et al., Zeit. f. Phys. B **99**, 163 (1996).
- [15] C. Palassis et al., Synth. Met. **120**, 999 (2001).
- [16] M. Mola et al., Rev. Sci. Instrum. **71**, 186 (2000).
- [17] M. Tamura et al., J. Phys. Soc. Jpn. **60**, 3861 (1991).

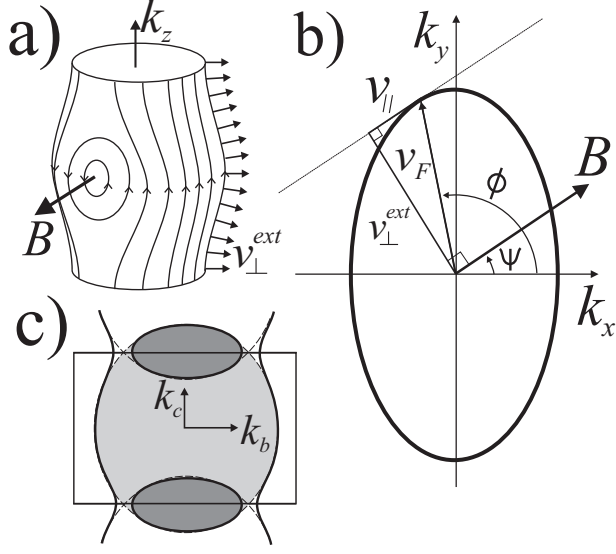


FIG. 1: (a) An illustration of the quasiparticle trajectories on a warped Q2D FS cylinder for a field oriented perpendicular to the cylinder axis; the warping has been greatly exaggerated for clarity. The resulting trajectories lead to a weak modulation of the quasiparticle velocities parallel to k_z and, hence, to a resonance in σ_{zz} . (b) The thick line shows $v_F(\phi)$ according to Eq. 1; the right angle triangle illustrates the relationship between $v_{\perp}^{ext}(\psi)$ and $v_F(\phi)$ (see text and Eq. 4 for explanation). (c) The Fermi surface of κ -(BEDT-TTF) $_2$ I $_3$ according to Ref. [13].

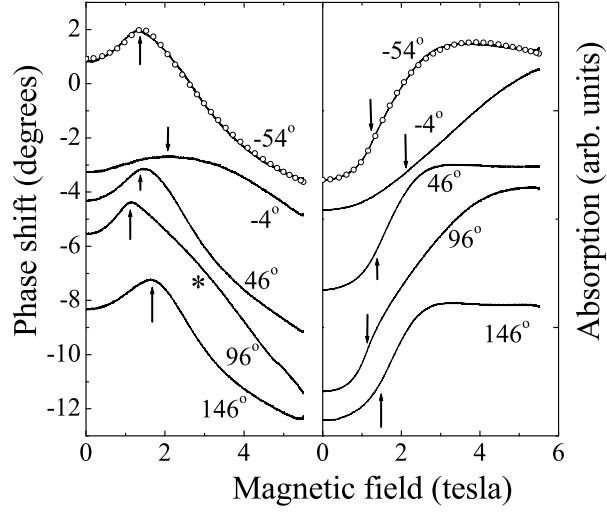


FIG. 2: Field dependence of the microwave phase shift (left) and absorption (right) for different field orientations (ψ). The solid curves represent the experimental data, while fits to the -54° data are shown by open circles. Arrows mark the resonance positions (B_{res}) determined from fits to Eq. 5; the asterisk marks a possible Q1D resonance.

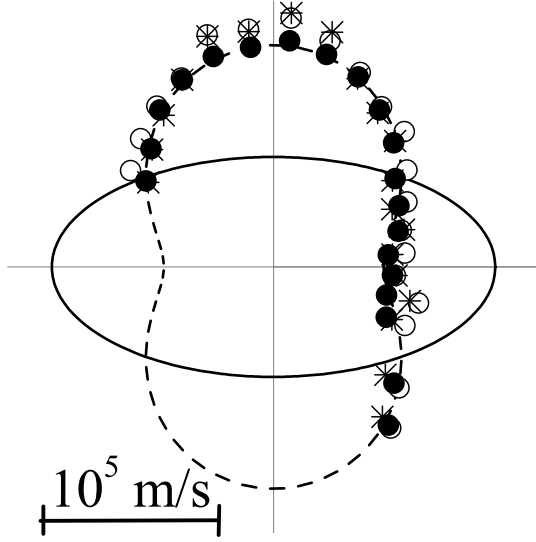


FIG. 3: Polar plot of $v_{\perp}^{ext}(\psi)$ obtained by three different methods: (1) from the maximum phase shift (●); (2) from fits to the absorption traces (○); and (3), from the fits of the phase shift traces (*). The dotted line is a fit to the points deduced by method 1, and the solid line is the resultant Fermi velocity, $v_F(\phi)$.